Mar. Fresh. Behav. Physiol., December 2003, Vol. 36, No. 4, pp. 307–319

ANALYSIS OF THE FLOW FIELD OF THE KRILL, *EUPHAUSIA PACIFICA*

JEANNETTE YEN[a,*], JASON BROWN[a] and DONALD R. WEBSTER[b]

[a]*School of Biology, Georgia Institute of Technology, Atlanta, Georgia, 30332;*
[b]*School of Civil and Environmental Engineering, Georgia Institute of Technology, Atlanta, Georgia, 30332*

(Received 26 December 2002; In final form 6 June 2003)

Velocity measurements were performed for the flow field generated by tethered krill *Euphausia pacifica*. The particle image velocimetry (PIV) technique was used to measure the velocity field in vertical planes aligned with the krill body axis. The krill generates a narrow jet-like flow behind and below the pleopods (roughly 25° below horizontal). The volume of fluid moving at greater than 10% of the maximum velocity near the pleopods is roughly 18 times larger than the volume of the krill. Thus, the hydrodynamic disturbance occupies a significantly larger region than the animal body. Other krill, sensing the flow disturbance, may take advantage of the flow induced by a neighbor to locate a mate or to draft for efficient propulsion.

Keywords: Krill; *Euphausia pacifica*; Flow field; Particle image velocimetry; PIV; Pleopods; Hydrodynamics

INTRODUCTION

Euphausiid krill play a major role in marine ecosystems (Loeb *et al*., 1997; Mangel and Nicol, 2000; Siegel and Nicol, 2000), serving as prey of larger predators such as birds and whales (Brodie *et al*., 1978; Veit *et al*., 1993; Nevitt, 2000) and as consumers of phytoplankton (Daly and Smith, 1993; Quetin *et al*., 1994). The capability of the larger species to form high-biomass schools (Hamner *et al*., 1983, Hamner *et al*., 1989; Ritz, 2000) can improve the efficiency of predator harvest and euphausiids are often targeted as a food source for fisheries (Nicol and Endo, 1999; Hewitt *et al*., 2002). Thus, understanding the physiochemical communication mechanisms among krill is critically important for an appreciation of species behavior as well as fishery management.

To find food, orient to neighbors, and avoid predators, krill need to perceive signals in their surrounding fluid environment. Krill show a variety of responses (see Nicol, 2003) that may be mediated by signals of different modalities: orientation, schooling and swarming (Hamner *et al*, 1983; O'Brien, 1989; Watkins and Murray, 1998; Folt

*Corresponding author. E-mail: jeannette.yen@biology.gatech.edu

ISSN 1023-6244 print: ISSN 1029-0362 online
DOI: 10.1080/1023624031000161439

and Burns, 1999), migration (Bollens *et al.*, 1992; De Robertis *et al.*, 2000), area-restricted search (Price, 1989; Hamner and Hamner, 2000), avoidance (O'Brien, 1987), molting (Hamner *et al.*, 1983; Buchholtz *et al.*, 1996), and movement of specific appendages (eye stalks; Land, 1980; thoracic basket; Hamner, 1988; flipped tail; O'Brien and Ritz, 1988). Although the presence of photophores and wavelength-sensitive eyes (Land, 1980; Frank and Widder, 1999) confirm sensitivity to visual signals, light is not always available. Other sensory modalities, such as chemoreception and fluid mechanoreception, can provide krill with information about their external environment. In the presence of phytoplankton patches, krill perform an area-restricted search (Price, 1989). In odor trails, krill change the rate of compression filtration of the feeding basket and increased their area-intensive turning (Hamner and Hamner, 2000). Physiological studies show threshold sensitivities of antennulary mechanoreception sensors to be on the order of μm of displacement and mm s^{-1} of fluid flow for *Euphausia superba*, which may enable krill to sense the shear layers of the propulsion jets of neighboring krill (Wiese and Marschall, 1990; Wiese and Ebina, 1995). Krill located downstream may gain a propulsion advantage from the momentum of the neighbor's jet flow (Ritz, 2000).

In order to evaluate hypotheses regarding mechanoreception, it is necessary to define the flow signals created and perceived by krill. An understanding of the fine-scale structure of the flow field generated by krill can provide information on the hydrodynamic and chemical signals in the vicinity of the individual to complement behavioral and physiological studies. This allows predictions to be made and hypotheses tested as to where and when behavioral interactions of krill may be effective. The feeding current is created by the expansion and compression of the thoracic legs (Hamner *et al.*, 1989) and a propulsive jet is created by the metachronal beat of the five pairs of swimmerets or pleopods of the krill (Kils, 1981). When they sweep these feeding and locomotory appendages through the surrounding fluid medium, a jet-like flow is formed. In this study, we perform laboratory measurements of living krill to quantify the velocity gradients in the flow generated by moving pleopods of the euphausiid, *Euphausia pacifica*.

METHODS

Euphausia Pacifica

Individuals were collected in Santa Barbara Basin, a coastal basin at latitude 34.20 N 120.00 W in the eastern Pacific Ocean. Intact living specimens were sorted into 2 L containers of seawater and placed in an insulated cooler with ice packs. Coolers were either hand-carried or mailed overnight to the laboratory at the Georgia Institute of Technology in Atlanta. Animals were kept in the dark in a 12°C environmental chamber in 1-gallon glass jars with gentle aeration and fed a mixture of *Rhodomonas* and *Artemia* nauplii. Under these conditions, *E. pacifica* remained active for over two months.

During the flow measurements, an individual krill was tethered onto a thin steel wire using super glue. The wire was supported by a 3-axis precision position manipulator. The tethered krill was submerged in a clear acrylic cubic tank, 15 cm on a side, filled with artificial seawater with 35 ppt. The walls of the saltwater tank appeared

to have a negligible effect on the flow field of the krill. The temperature of the seawater was maintained at 12°C by immersing the cube in a recirculating cold freshwater bath. The bath also was constructed with clear acrylic walls to facilitate optical access.

Flow Visualization and Characterization

Velocity measurements were performed using the nonintrusive particle image velocimetry (PIV) technique (e.g. Westerweel, 1997; Raffel *et al.*, 1998). The technique determines the velocity field of a fluid by measuring the displacement of very small suspended particles over a brief time interval. The particles are assumed to closely follow the flow over short time intervals, thus their motion corresponds to the fluid velocity.

In the current experiments, titanium dioxide particles with a mean diameter of less than 5 μm were used as the flow tracer. The particle locations were determined by photographing scattered laser light. Illumination of the tracer particles was provided by dual pulsed Nd:YAG lasers (monochromatic light with 532 nm and a maximum pulse energy output of 130 mJ). The laser beam passed through a series of lenses and into the saltwater tank to form a 1 mm thick sheet of light at the krill. A digital camera (8 bit, 1008×1018 pixels) aimed perpendicularly at the light sheet imaged the laser light scattered from the particles. The image acquisition was performed in a dark environment with the laser providing the only light, thus the PIV images consisted of bright particle spots against a dark background. A precision timing control circuit synchronized the camera shutter and laser pulses such that two consecutive exposures are acquired, Δt seconds apart, with one laser pulse per image. The time between consecutive laser pulses, Δt, varied from 2 to 25 ms, depending on which plane of the flow field was being illuminated (because resolving higher velocities required shorter delays). The camera acquired 10 image pairs per second. Images from the camera were captured and stored for subsequent analysis on a Windows-based PC.

To minimize the optical disturbance of the krill, the laser output energy was adjusted to the lowest level that provided good quality images for PIV. The krill appeared to be disturbed when a sequence of laser pulses was initiated or terminated; thus the laser pulsed continuously during the experiment.

The digital images were interrogated by a cross correlation procedure to determine the particle displacement (Westerweel, 1997). A 32×32 subwindow in the first image was correlated with the corresponding subwindow in the paired image. The location of the peak in the correlation function was determined to subpixel accuracy and corresponded to the average displacement of the group of particles in the subwindow. The displacement field over the area of the image was estimated by repeating this process for each location in a grid defined by 50% overlap of the subwindows. Combining the displacement estimate with the image magnification and time interval between laser pulses yielded the local velocity. Derivative properties, such as the vorticity, were then calculated directly from the velocity field using a central finite-difference scheme.

A coordinate system was defined such that X is the horizontal direction parallel to the krill body axis, Y is transverse to the body axis, and Z is the vertical direction. The origin of the coordinate system is located at the midpoint of the body width at the eye location. In this article, we present velocity fields for planes defined by the

X–*Z* coordinates. Measurements were collected for seven parallel planes corresponding to *Y* between 0 and 0.6 cm. Five sets of images, each consisting of 37 vector fields, were collected for each plane. Thus, over 180 velocity vectors were measured at each location in the field. Measurements were taken during the day between 10 and 60 min after tethering. Flow measurements were performed for several animals and the data from one specimen are presented here to represent a persistent flow produced by *E. pacifica* (2 cm = specimen length).

RESULTS

Spatial and Temporal Variations in the Velocity Field

The flow generated by this crustacean was directed downward and to the rear of the organism in the midline plane ($Y = 0$; Fig. 1). The magnitude and directionality of the instantaneous velocity field (Fig. 1A) was similar to the field averaged over a time interval of 3.2 s (Fig. 1B). The krill-generated flow resembled a jet, defined by a high speed core of flow in a narrow region (Fig. 2A). The angle of the jet relative to the horizontal direction was roughly 25°. Over the time period analyzed for the average vector field, the pleopods remained in motion and the jet-like flow persisted. The largest velocity in the region near the pleopods was in the range of $4.86 \pm 1.10\,\mathrm{cm\,s^{-1}}$. The velocity fluctuations were greatest in the region of maximum flow (Fig. 2C). The local turbulence intensity, defined by the ratio of the standard deviation to the local mean velocity magnitude (Fig. 2D), was greatest in the shear layers of the jet (nearly 40%) compared to less than 10% in the jet core.

The flow speed decreased rapidly in all directions from the location of maximum velocity just below the pleopods (Fig. 2B). For instance, in the posterior direction towards the tail (0°), the flow declined to 10% of the maximum flow speed ($\sim 5\,\mathrm{mm\,s^{-1}}$) at a distance 1.19 cm (Table I, Fig. 3). The corresponding distance along the other profiles shown in Fig. 3 are reported in Table I. The slowest rate of decrease was along the axis of the jet (335°), for which the 10% contour extended beyond the field of view of the camera. By fitting the flow speed values to an exponential decay curve, we estimated that the flow declines to approximately $5\,\mathrm{mm\,s^{-1}}$ at 3.7 cm, which corresponds to nearly two bodylengths. In contrast, at right angles to the jet (i.e. 245°) the flow decreased to 10% of the maximum in less than 1.0 cm from the region of maximum speed (Table I).

In the transverse direction (*Y*-direction), the speed of the flow decreased rapidly away from the region of maximum flow (Table II). The flow decreased to 10% of the maximum flow speed at a distance 0.23 cm.

Vorticity Field

Figure 4 shows the mean vorticity field. The negative and positive bands of vorticity coincide with the shear layers at the edges of the jet-like flow (see Fig. 1B). A bifurcated jet structure is revealed by the double band of negative vorticity along the lower edge of the jet-like flow. The bifurcating structure also is observed in the vector field (Fig. 1B).

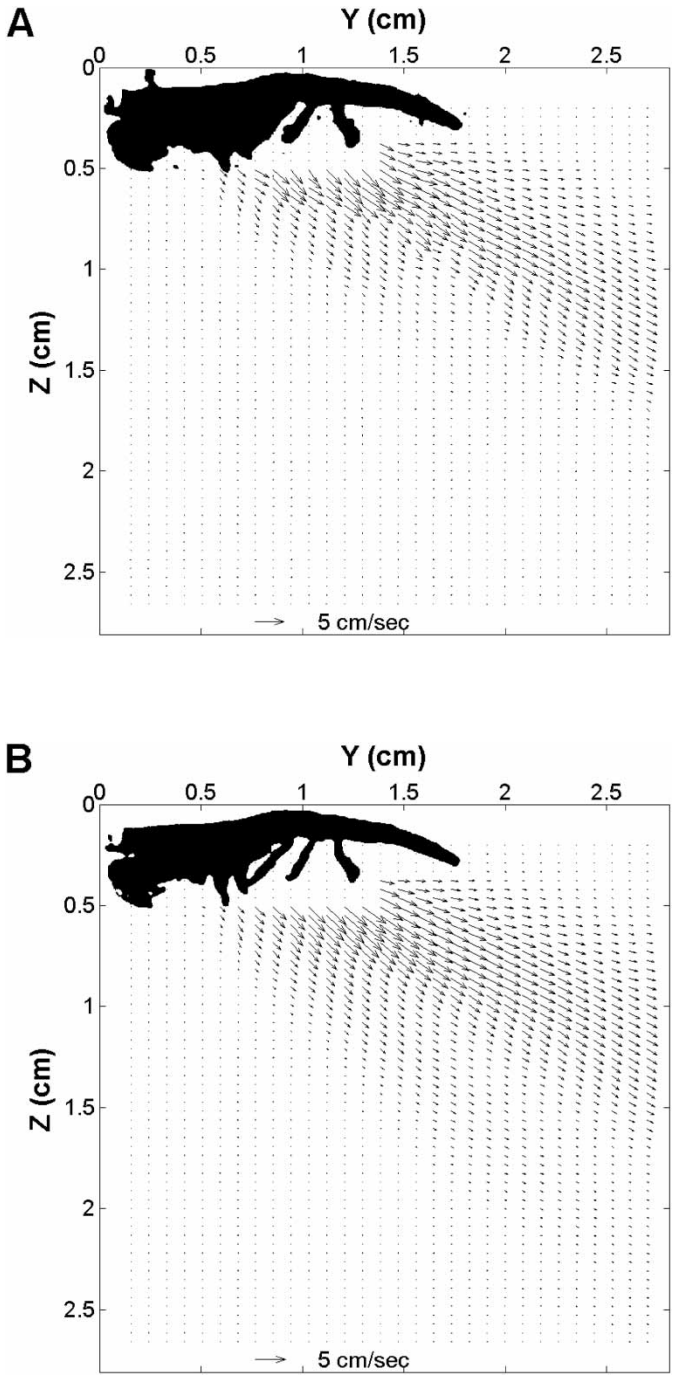

FIGURE 1 (A) The instantaneous velocity vector field in a longitudinal plane of flow generated by the krill *Euphausia pacifica*. The plane shown corresponds to the midline of the krill body (i.e. $Y=0$). Maximum instantaneous velocity in this figure is $5.1\,\mathrm{cm\,s^{-1}}$. (B) The average velocity vector field for the same conditions shown in (A), calculated from 5 sets of vector fields, each collected over a period of 3.2 s, for a total of 183 fields. Maximum average velocity is $4.9\,\mathrm{cm\,s^{-1}}$. This field shows a bifurcated jet with a stronger flow immediately below the tail and a weaker stream below.

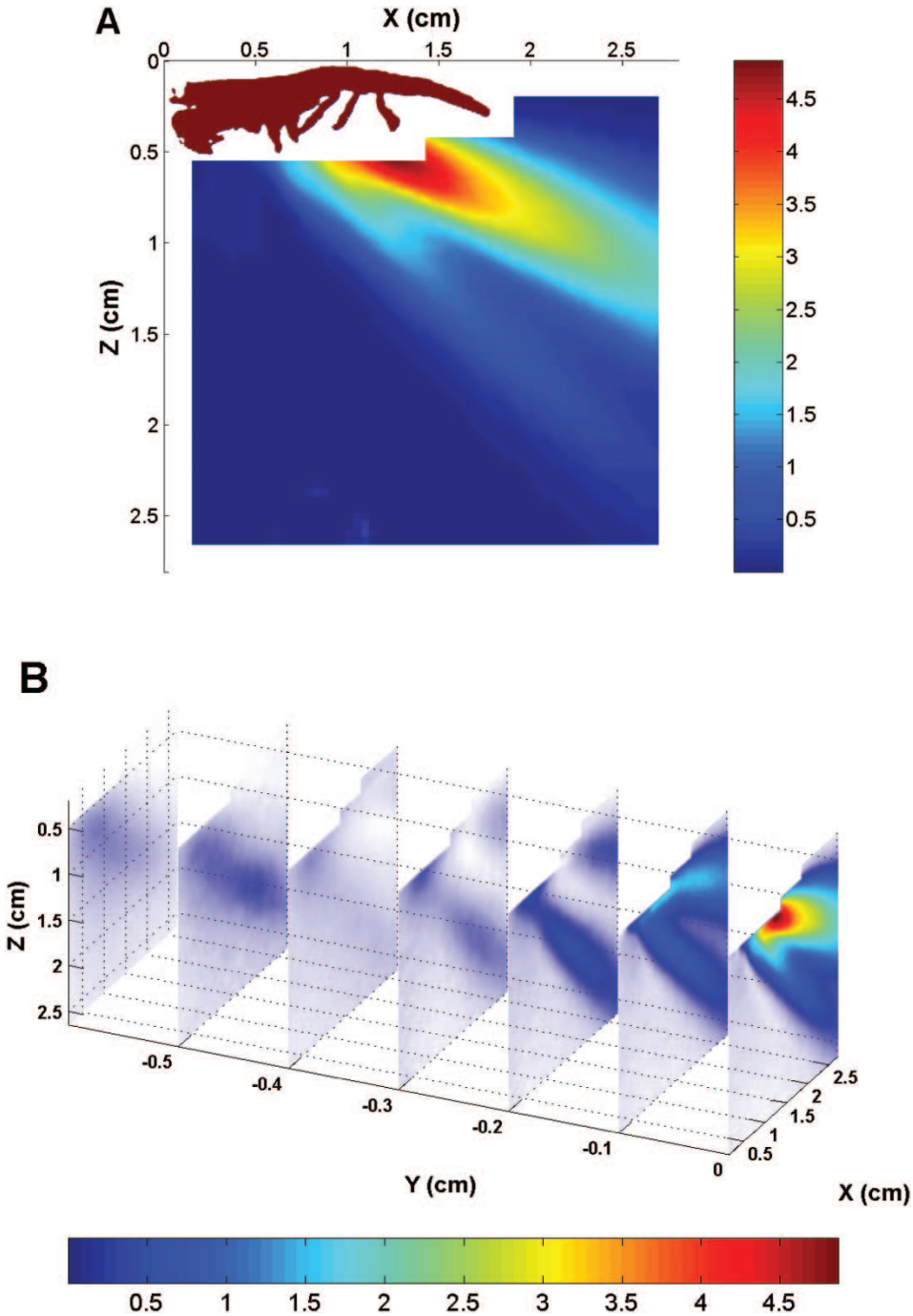

FIGURE 2 (A) Contours of the average flow speed, in $\mathrm{cm\,s^{-1}}$, along the midline (i.e. $Y=0$) of the flow generated by the krill *Euphausia pacifica*. (B) Multiple planar slices of the average flow speed, in $\mathrm{cm\,s^{-1}}$, separated by 1 mm in the transverse (Y) direction. Contours below $0.35\,\mathrm{cm\,s^{-1}}$ are transparent to better emphasize the low-speed flow features. (C) Standard deviation, in $\mathrm{cm\,s^{-1}}$, of the flow speed in the $Y=0$ plane. (D) Local turbulence intensity, defined by the percentage of the standard deviation compared to the local mean speed, in the $Y=0$ plane.

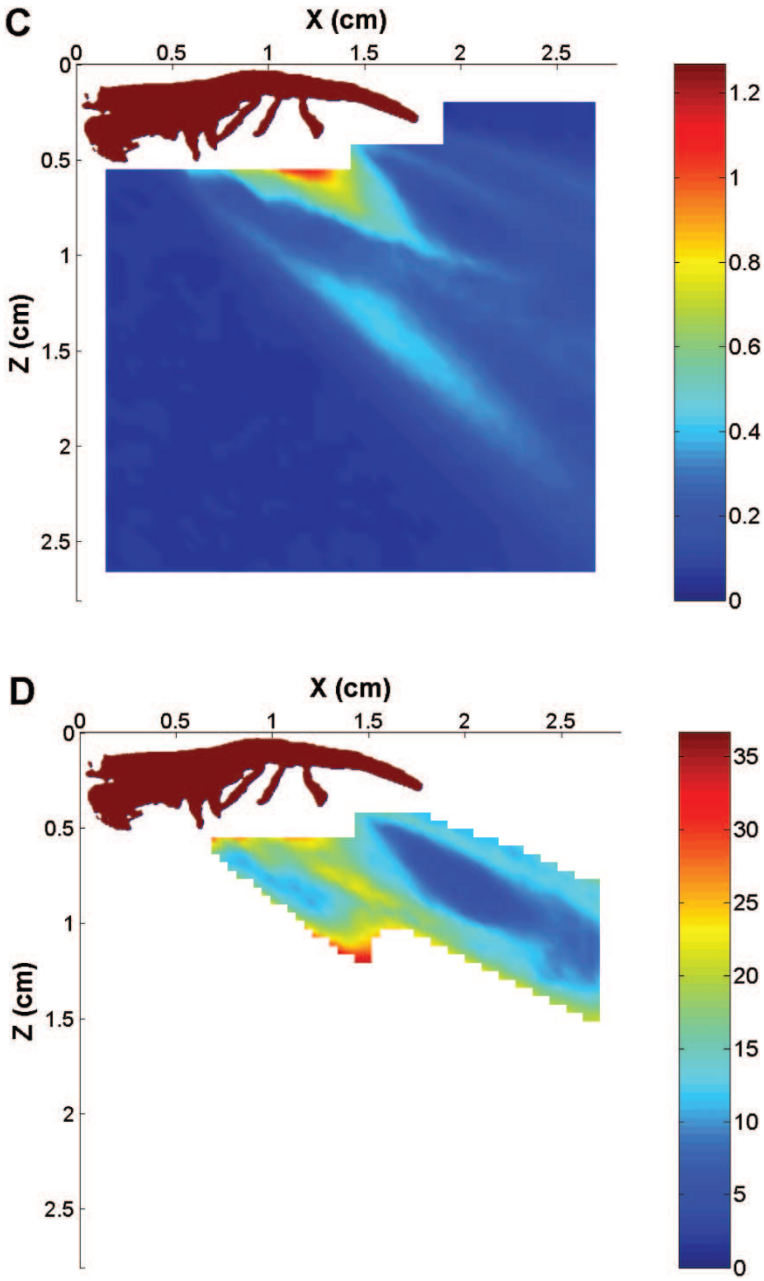

FIGURE 2 Continued.

DISCUSSION

The tethered krill *E. pacifica* uses its pleopods and urosome to form a narrow asymmetric jet-like flow feature, with a high-speed core flanked by shear layers. Acting as vanes, the appendages direct the flow in a narrow jet oriented downward at a shallow

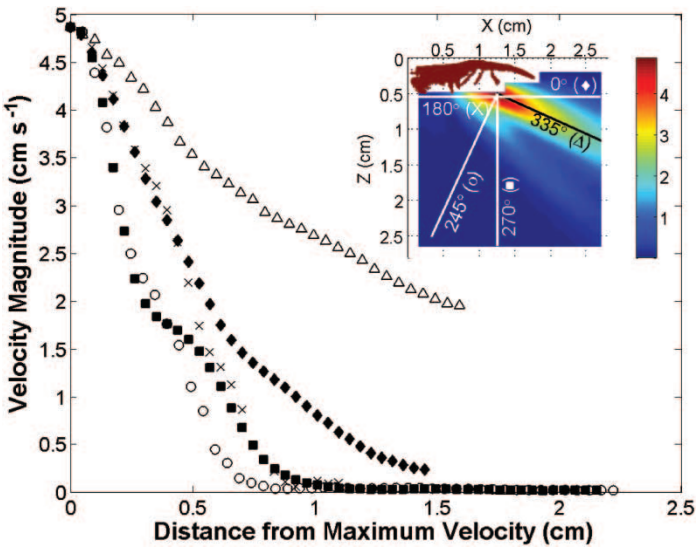

FIGURE 3 Profiles of flow speed generated by the krill *Euphausia pacifica* at the midline (i.e. $Y=0$). The coordinate system is defined in the inset, which is a reproduction of Fig. 2(A). Profiles are shown for five coordinate directions: along the axis of the body posteriorly (0°, ◆) and anteriorly (180°, ×), along the vertical axis (270°, ■), along the jet centerline (335°, △) and at a right angle to the jet centerline (245°, ○). Hollow symbols represent data interpolated between grid points. An exponential function was fit to each profile (see Table I).

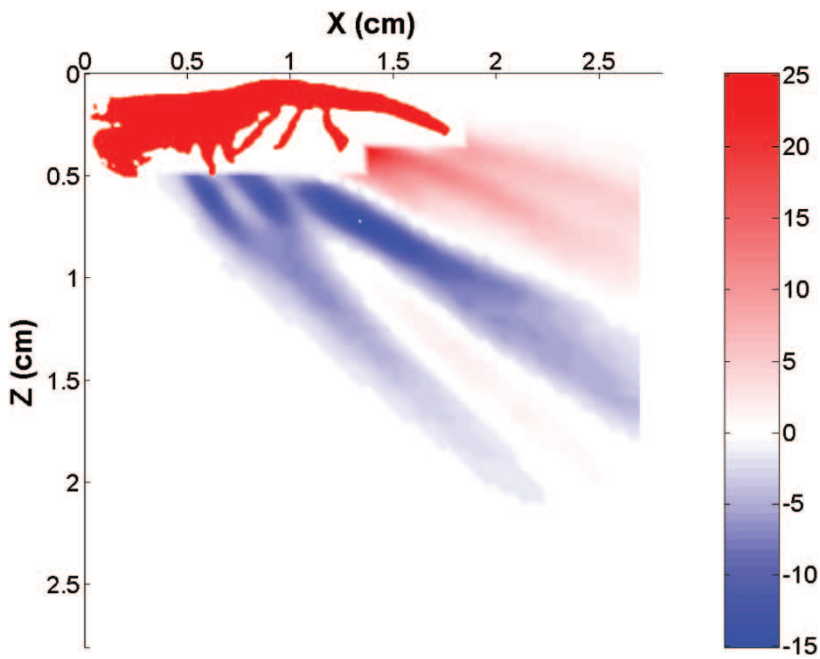

FIGURE 4 The average vorticity field corresponding to the krill-generated flow field. The bands of positive and negative vorticity correspond to the shear layers in the jet-like flow. Vorticity units are s^{-1}.

TABLE I The profiles of velocity magnitude (Fig. 3) were fitted to an exponential function: $|U| = |U_{max}|e^{-\beta\xi}$, where $|U|$ is the velocity magnitude and ξ is the distance from the location of maximum velocity. Tabulated for the profiles shown in Fig. 3 are the exponential coefficient β and the location at which the flow speed is 10% of the maximum ($r^2 > 0.99$). Profile data show the decline in flow speed in six directions: along the axis of the body posteriorly (0°) and anteriorly (180°), along the vertical axis just below the pleopods (270°), along the axis of the jet (335°) and at right angles to the axis of jet (245°), and also in the transverse direction

Profile direction	β	*Distance* (cm) *for 10% of* $\lvert U_{max}\rvert$
0	1.79	1.19
180	2.32	0.75
245	5.5	0.94
270	2.9	0.75
335	0.6	3.8
Transverse	10.1	0.23

TABLE II The maximum average speed at each transverse plane decreases with distance from the midplane. The location at which the flow speed is 10% of the maximum is 0.23 cm ($\beta = 10.1$; $r^2 > 0.99$)

Transverse distance (cm) *from midline*	*Speed* $\lvert U\rvert$ ($cm\,s^{-1}$)	*Standard deviation* ($cm\,s^{-1}$)
0	4.86	1.10
0.1	1.81	0.63
0.2	0.52	0.22
0.3	0.26	0.09
0.4	0.16	0.07
0.5	0.28	0.07
0.6	0.18	0.07

angle of 25° to the rear of the animal. For a freely swimming krill the downward angle of the jet may minimize sinking (Miyashita *et al*., 1996). The few records that we have obtained for freely swimming *E. pacifica* (Brown and Yen, unpubl.) suggest that the jet is narrower and has a smaller spatial extent overall. For the flow field of the tethered *E. pacifica* presented here, the velocity is maximum near the reciprocating pleopods. The speed decreases rapidly to either side of the krill (to less than 10% of the maximum within 2 mm) and directly below and behind the krill (within one bodylength). However, along the core of the jet, the flow remains above 10% of the maximum nearly two bodylengths downstream.

A comparison of the cylindrical volume occupied by the krill (volume of krill $\approx \pi r^2 \ell = 0.14\,cm^3$, where r = radius of krill ≈ 0.15 cm and ℓ = krill length ≈ 2 cm) to the elliptical cylinder volume occupied by the biologically-generated jet enclosed within the 10% velocity contour (volume of flow field $= (\pi ab)\ell \approx 2.4\,cm^3$, where $a = 0.94$ cm and $b = 0.23$ cm are the major and minor semi-axes of the elliptical cross-section and ℓ = distance for 10% of $U_{max} \approx 3.7$ cm) shows that the krill influences a fluid volume that is roughly 18 times larger than its own body. Another animal, detecting the flow, would remotely respond to the hydrodynamic field that the krill creates. Evidence of the response to hydrodynamic disturbances includes swarming

copepods, which appear to separate by the width of their feeding current rather than by the width of their bodies (Leising and Yen, 1997). Because the flow feature of *E. pacifica* is asymmetric relative to the body axis, we predict that krill sensing each other will be positioned asymmetrically. Transversely, krill would need to be very near to affect each other because of the rapid velocity decrease in that direction. The jet in the downstream direction transmits more information regarding the size and speed of the source krill, or any emitted chemicals (e.g. Atkinson and Whitehouse, 2000). To acquire this information without loss of directionality, the optimal position may be in the jet core. Krill spaced two bodylengths below a neighbor along the direction of the central core of the jet would be subject to flow speeds of roughly $5\,\mathrm{mm\,s^{-1}}$. Because flows of this magnitude are within the range of possible threshold sensitivities of mechanoreceptive antennulary setae (Weissburg *et al.*, unpubl.), krill in this formation should be able to detect their neighbors. Field observations are needed to measure nearest neighbor distances to quantify asymmetry of the spacing and assess the influence of adjacent flow fields of krill.

For *E. superba* O'Brien (1987) observed a preference for positions behind and roughly 45° above and below its nearest neighbors (NN). Neighbors to the side had significantly smaller NN distances (NND) than neighbors positioned in front or behind. These observations indicate an asymmetry of spacing and the possible influence of the hydrodynamic field on the aggregate behavior of krill. O'Brien (1987) suggests that pelagic schools may have small NND to ensure continual contact with conspecifics and hence a possible spatial reference in the absence of a benthic substrate.

The mean pathlines show trajectories for fluid entrained toward the krill and exiting within the jet (Fig. 5). Using the width of the jet-like flow (~1 cm) and the velocity just below the pleopods, the Reynolds number of the krill flow field is roughly 175. Flow at this Re is neither creeping ($\mathrm{Re} < 1$) nor fully turbulent ($\mathrm{Re} > 4000$). However, the turbulence intensity in the shear layers is up to 40%, thus the flow in this region should be considered turbulent. The entrainment flow approaching the animal is much smoother and quiescent. The smooth incoming flow expands the krill sensory field beyond the physical extent of its sensors. Signals, advected by the entrainment flow and detected by antennulary sensors, may originate at spatially defined locations in the incoming flow. Mouthparts are receiving input from flow arriving from specific sectors of the volume of water entrained in front of the krill. Information, in the form of hydrodynamic disturbances, may mediate orientation behavior in a freely swimming individual. By generating this flow, the organism is able to gather information about food or signals from a volume larger than that mapped by a static measure of the fluid adjacent to the antennulary sensors or mouthparts. Furthermore, by advecting the fluid, the krill increases the rate of information acquisition instead of relying on the slow process of diffusion. Both processes: maintaining quiescent entrainment flow with predictable positions of pathlines and creating advection in the flow field, enhance its sensory field.

The coordinated movements and positioning of the pleopods and the urosome create a focused narrow jet not much wider than the organism itself and similar to the span of the antennulary sensors. A krill tracking another krill may extract information from the jet with high momentum and mass transport and may not need to cast widely to discern the edges of the jet. The receiver may be a schoolmate searching for the drafting location where the efficiency of swimming is optimal, hence deriving the highest energy advantage from schooling. Alternatively, the receiver may be a mate, assessing

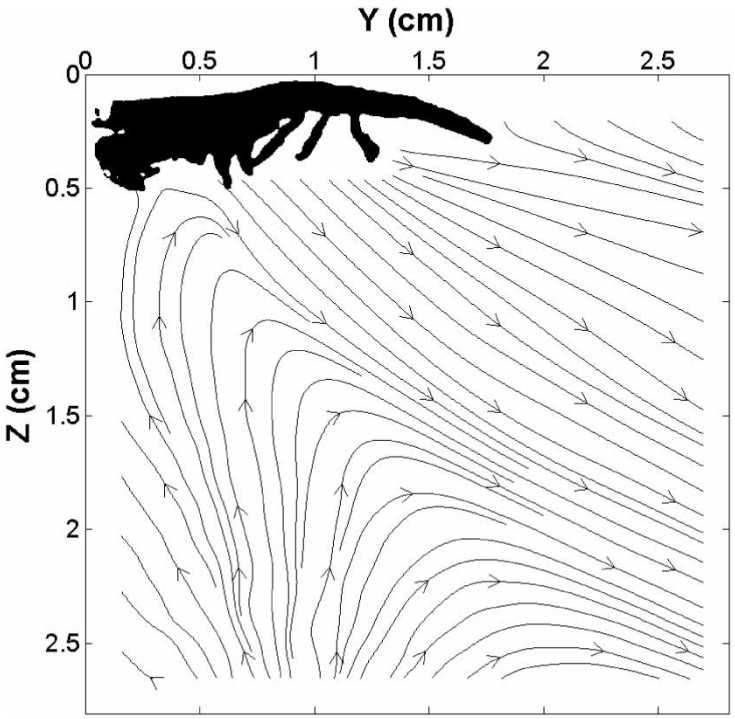

FIGURE 5 Pathlines for the average velocity field. The pathlines show water entrained from below near the front of the organism and ejected downward behind the organism.

the identity of the sender by the chemical composition or fluid structure of the jet. Krill are known to respond to chemical odorants (Price, 1989) and have displayed some narrow casting as part of the tracking behavior (Hamner and Hamner, 2000). By creating a spatially narrow signal, the sender may minimize detection by a predator with large or widely spaced sensors that may not be able to discern such spatially discrete flow or odor patterns. In other words, the information in the hydrodynamic signal may be receiver-specific.

To summarize this analysis of the krill *E. pacifica* and its flow field, we note that the interaction of an aquatic organism with water-borne food or signals is defined not only by characteristics of the organism but also by the characteristics of the adjacent fluid environment (e.g. Yamazaki *et al.*, 2002). Over evolutionary time, the sensitivity of the receptors can be honed to detect appropriate intensities and frequencies of hydrodynamic signals or species-specific chemical structures of the signal. The design of the sensor can enhance encounters with incoming signals. Similarly, the form of the food gathering appendage can evolve to improve handling efficiency of preferred prey and the collection of signals. Furthermore, the features of the induced flow field and hydrodynamic signals can change and adapt. Here, we find *E. pacifica* creates a smooth intake directed towards its mouthparts and sensors, hence employing the entrainment flow field as its sensory space. These flow structures confer benefits that enhance food-gathering and signal-processing by the euphausiid. By directing the exit flow in a narrow focused jet, the krill generates a propulsive force. The propulsive jet also makes a conspicuous hydrodynamic signal that can reveal the location of the

krill to predators. Yet the narrow jet is less wide than the sensor span of certain larger predators, which may reduce detection of this outgoing signal disturbance. In contrast, the narrowness of the jet may work well for information transmission between krill because the span of the jet matches the span of the antennulary sensors. By focusing the flow into an intense and asymmetric jet, a potential communication channel is created. Krill, capable of sensing flow or chemicals transported in the flow field, can maximize the distance of detection by positioning themselves along the direction of the core of the jet. An assessment of schooling advantages may rely more on a measure of the vertical rather than the lateral separation distances between individuals. Behavioral analyses of krill *in situ* are needed to determine if the positions of adjacent krill reflect the directionality of the induced flow field. In addition, neurophysiological studies are needed to assess threshold sensitivities to test the hypothesis that krill perceive each other by signals transmitted in their induced flow field.

Acknowledgments

We would like to thank Dr. Steve Nicol for inviting us to and Dr. So Kawaguchi for hosting us at the International Workshop on Understanding Living Krill for Improved Management and Stock Assessment, held in Nagoya, Japan, in October 2002. We appreciate the review and insightful comments of Drs. David Ritz, Atsushi Tsuda, and Langdon Quetin. We give much appreciation to Sarah Goldthwait for collecting and shipping the Pacific krill and to Yin Chang for taking care of them. This research was supported by a collaborative National Science Foundation grant OCE-0296101 to Alice Alldredge and J. Yen.

References

Atkinson, A. and Whitehouse, M.J. (2000). Ammonium excretion by Antarctic krill *Euphausia superba* at South Georgia. *Limnol. Oceanogr.*, **45**, 55–63.

Bollens, S.M., Frost, B.W. and Lin, T.S. (1992). Recruitment, growth, and diel vertical migration of *Euphausia pacifica* in a temperate fjord. *Mar. Biol.*, **114**, 219–228.

Brodie, P.F., Sameoto, D.D. and Sheldon, R.W. (1978). Population densities of euphausiids off Nova Scotia as indicated by new sample, whale stomach contents and sonar. *Limnol. Oceanogr.*, **23**, 1264–1267.

Buchholz, F., Watkins, J.I., Priddle, J. and Morris, D.J. (1996). Moult in relation to some aspects of reproduction and growth in swarms of Antarctic krill, *Euphausia superba*. *Mar. Biol.*, **127**, 201–208.

Daly, K.L. and Smith, W.O. (1993). Physical-biological interactions influencing marine plankton production. *Annu. Rev. Ecol. Syst.*, **24**, 555–585.

De Robertis, A., Jaffe, J.S. and Ohman, M.D. (2000). Size-dependent visual predation risk and the timing of vertical migration in zooplankton. *Limnol. Oceanogr.*, **45**, 1838–1844.

Folt, C.L. and Burns, C.W. (1999). Biological drivers of zooplankton patchiness. *Trends Ecol. Evol.*, **14**, 300–305.

Frank, T.M. and Widder, E.A. (1999). Comparative study of the spectral sensitivities of mesopelagic crustaceans. *J. Comp. Physiol. A*, **185**, 255–265.

Hamner, W.M. (1988). Biomechanics of filter feeding in the Antarctic krill *Euphausia superba*: review of past work and new observations. *J. Crust. Biol.*, **8**, 149–163.

Hamner, W.M., Hamner, P.P., Strand, S.W. and Gilmer, R.W. (1983). Behavior of Antarctic krill, *Euphausia superba*: chemoreception, feeding, schooling, and molting. *Science*, **220**, 433–435.

Hamner, W.M., Hamner, P.P., Obst, B.S. and Carlton, J.H. (1989). Field observations on the ontogeny of schooling of *Euphausia superba* furciliae and its relationship to ice in Antarctic waters. *Limnol. Oceanogr.*, **34**, 451–456.

Hamner, W.M. and Hamner, P.P. (2000). Behavior of Antarctic krill (*Euphausia superba*): schooling, foraging, and antipredatory behavior. *Can. J. Fish. Aquat. Sci.*, **57**, 192–202.

Hewitt, R.P., Watkins, J.L., Naganobu, M., Tshernyshkov, A.S., Brierley, A.S., Demer, D.A., Kasatkina, S., Takao, Y., Goss, C., Malyshko, A., Brandon, M.A., Kawaguchi, S., Siegel, V., Trathan, P.N., Emery, J.H., Everson, I., Miller, D.G.M. (2002). Setting a precautionary catch limit for Antarctic krill. *Oceanogr*., **15**, 26–33.

Kils, U. (1981). The swimming behaviour, swimming performance and energy balance of Antarctic krill, *Euphausia superba*. *Biomass Sci. Ser*., **3**, 1–121.

Land, M.F. (1980). Eye movements and the mechanism of vertical steering in euphausiid crustacea. *J. Comp. Physiol*., **137**, 255–265.

Leising, A. and Yen, J. (1997). Spacing mechanisms within light-induced copepod swarms. *Mar. Ecol. Prog. Ser*., **155**, 127–135.

Loeb, V., Siegel, V., Holm-Hansen, O.R., Hewitt, R., Fraser, W., Trivelpiece, W. and Trivelpiece, S. (1997). Effects of sea-ice extent and salp or krill dominance on the Antarctic food web. *Nature*, **387**, 897–900.

Mangel, M. and Nicol, S. (2000). Krill and the unity of biology. *Can. J. Fish. Aquat. Sci*., **57** (Suppl. 3), 1–5.

Miyashita, K., Aoki, I. and Inagaki, T. (1996). Swimming behaviour and target strength of isada krill (*Euphausia pacifica*). *ICES J. Mar. Sci*., **53**, 303–308.

Nevitt, G. (2000). Olfactory foraging by Antarctic Procellariiform seabirds: life at high Reynolds numbers. *Biol. Bull*., **198**, 245–253.

Nicol, S. (2003). Living krill, zooplankton and experimental investigations: A discourse on the role of krill and their experimental study in marine ecology. *Mar. Fresh. Behav. Physiol*., **36**, 191–205.

Nicol, S. and Endo, Y. (1999). Krill fisheries: Development, management and ecosystem implications. *Aquat. Living Resour*., **12**, 105–120.

O'Brien, D.P. (1987). Description of escape responses of krill (*Crustacea*, *Euphausiacea*), with particular reference to swarming behavior and the size and proximity of the predator. *J. Crustacean Biol*., **7**, 449–457.

O'Brien, D.P. (1989). Analysis of the internal arrangement of individuals within crustacean aggregations (*Euphausiacea*, *Mysidacea*). *J. Exp. Mar. Biol. Ecol*., **128**, 1–30.

O'Brien, D.P. and Ritz, D.A. (1988). The escape response of gregarious mysids (Crustacea: Mysidacea): towards a general classification of escape responses in aggregated crustaceans. *J. Exp. Mar. Biol. Ecol*., **116**, 257–272.

Price, H.J. (1989). Swimming behavior of krill in response to algal patches: A mesocosm study. *Limnol. Oceanogr*., **34**, 649–659.

Quetin, L.B., Ross, R.M. and Clarke, A. (1994). Krill energetics: seasonal and environmental aspects of the physiology of *Euphausia superba*. In: El-Sayed, S.Z. (Ed.), *Southern Ocean Ecology: The BIOMASS Perspective*, pp. 165–184. Cambridge University Press, Cambridge.

Raffel, M., Willert, C. and Kompenhans, J. (1998). *Particle Image Velocimetry – A Practical Guide*. Springer-Verlag, New York.

Ritz, D.A. (2000). Is social aggregation in aquatic crustaceans a strategy to conserve energy? *Can. J. Fish. Aquat. Sci*., **57**, 59–67.

Siegel, V. and Nicol, S. (2000). Population parameters. In: Everson, I. (Ed.), *Krill Biology, Ecology and Fisheries*, pp. 103–149. Blackwell Science, Oxford.

TOS (2002).

Veit, R.R., Silverman, E.D. and Everson, I. (1993). Aggregation patterns of pelagic predators and their principal prey, Antarctic krill, near South Georgia. *J. Anim. Ecol*., **62**, 551–564.

Watkins, J.L. and Murray, A.W.A. (1998). Layers of Antarctic krill, *Euphausia superba*: are they just long krill swarms? *Mar. Biol*., **131**, 237–247.

Wiese, K. and Marschall, H.P. (1990). Sensitivity to vibration and turbulence of water in context with schooling in Antarctic krill, *Euphausia superba*. In: K. Wiese *et al*. (Eds.), *Frontiers in Crustacean Neurobiology*, pp. 121–130. Birkhauser Verlag, Basel.

Wiese, K. and Ebina, Y. (1995). The propulsion jet of *Euphausia superba* (Antarctic krill) as a potential communication signal among conspecifics. *J. Mar. Biol. Assoc. U.K*., **75**, 43–54.

Westerweel, J. (1997). Fundamentals of digital particle image velocimetry. *Meas. Sci. Technol*., **8**, 1379–1392.

Yamazaki, H., Mackas, D. and Denman, K.L. (2002). Coupling small-scale physical processes with biology. In: Robinson, A.R., McCarthy, J.J. and Rothschild, B.J. (Eds.), *The Sea*, Vol. 12, pp. 51–111. John Wiley and Sons, New York.